Wood Sci. Technol. 16: 241–259 (1982)

Wood Science and Technology

On the Fracture Morphology in Wood

Part 1: A SEM-Study of Deformations in Wood of Spruce and Aspen Upon Ultimate Axial Compression Load

L. J. Kučera and M. Bariska

Institut für Wald- und Holzforschung, Eidgenössische Technische Hochschule Zürich, Switzerland

Summary. Structural changes in spruce and aspen wood samples subjected to axial compression were examined by means of the scanning electron microscope. For comparison, macroscopic model experiments were carried out on tube-shaped samples made of paper so as to represent segments of fibriform xylem cells. The results show that there are fracture patterns characteristic of wood in general and others characteristic of the species of wood. The phenomena characteristic of wood in general are prevalent at the cellular level and in the fracture behaviour of the cell wall layers and perforations. The characteristics of the various species of wood dominate at the level of the growth rings and are decisively influenced by the composition and arrangement of the tissues. The model experiments show that the failure morphology of the individual cells of the xylem may be explained to some extent by their geometry.

Introduction

At first sight the failure process is a macroscopic phenomenon. However, the variable strength of the wood in any one species and the varying fracture behaviour in the different species cannot be completely explained by a macroscopic description of the wood. The reasons must be looked for in other levels of organization, chiefly in the macromolecular and microscopic ones. The present article will attempt to answer the question whether and to what extent the fracture behaviour of wood may be explained through its anatomical features. By comparing the fracture behaviour of different wood species upon axial loading an attempt is made to uncover fracture patterns characteristic of wood in general and of the species in particular. This is also the purpose of the model experiments in which the fracture behaviour of model samples made of paper is examined upon the same testing procedure and compared with that of the wood cells. The following questions are posed in connection with the fracture behaviour:

- What part does the tissue arrangement play?
- Can the fracture mechanism of the individual cell types be adequately explained on the basis of morphological parameters?

0043-7719/82/0016/0241/$ 3.80

– What is the mechanical function of the individual cell-wall layers and perforations, and is there a common pattern of response?

Material and Methods

The investigation was carried out on wood samples of Norway spruce (*Picea abies* Karst.) and Aspen (*Populus tremula* L.). The similarities and the differences of anatomical, physical and mechanical properties of these two species should make it possible to distinguish between fracture patterns which are characteristic of wood and those particular to the species.

The material had been taken from the experimental station of the ETH Zürich on a local mountain, called Uetliberg, at about 730 m above sea-level from a Gallio odorati-Fagetum typicum stand (Ellenberg, Klötzli 1972) with NNE exposure during the felling period 1978/79. Healthy mature trees were chosen and from their trunks parts without defects were selected for preparing the samples. The test samples with dimensions of 20 x 20 x 20 mm were sawn from the adult parts of a cross-section of the trunk. After drying and conditioning to 12% moisture content they were axially compressed in a testing apparatus according to DIN 52 185 until the length was reduced by 10%. During the preparation of the samples for examination under the scanning electron microscope (SEM), modification of deformation and fracture phenomena by possible swelling was carefully avoided. For the identification of additional deformations – possibly introduced by the preparation or already present in the standing tree – control samples were prepared from the same material, in exactly the same way as the test samples and examined under the SEM for detecting artefacts.

Compared with the usual SEM preparation techniques (Exley et al. 1974) some modifications were adopted with regard to the extraction of the rough cubes, the final cutting and the treatment of the surfaces to be studied: In the tested wood samples the parts with visible deformations were marked, and rough blocks measuring 8 x 8 x 8 mm were isolated from these pieces. To obtain the samples the wood was first split layer by layer in the longitudinal direction and then sawed across the grain with a fine handsaw. The samples were cut without any previous plasticization. Final cutting was carried out under a stereomicroscope, either by handcutting with razor blades or by microtome cutting; an exact description of the method and equipment used is to be found in Kučera (1981). The mounted samples were treated with conductive silver paint and dried in a vacuum oven at 50 °C and ca. 15 μbar vacuum over phosphorous pentoxide. A 40 nm thick gold layer was sputtered on at 0.15 mbar pressure of argon gas. The usual removal of residual cell contents and of possible contaminations with Eau de Javelle and acetic acid and the customary dehydration process with alcohol and acetone were omitted in order to avoid any changes of the fracture and deformation phenomena by swelling. The samples were so arranged in the SEM-column that the original axial orientation always appeared vertical on the screen. This applies to all the pictures reproduced.

For the construction of the tube-like test specimens that were considered as models for individual fibriform cell segments, paper was used. (Specific gravity: 80 g/m^2, quality: free of groundwood, material class 3 with 8–10 % extender, fully sized.) Nine model specimens were prepared with three different outer diameters (30, 60 and 90 mm respectively) and three wall portions (25, 50 and 75 % respectively) keeping the height of the specimens at 1 1/2 times the outer diameter. This experimental arrangement made it possible to see the dependance of the failure pattern on the dimensions of the specimens. The test specimens consisted of strips of paper of the appropriate widths tightly rolled up, but not glued together. The number of wall layers ranged between 22 and 250, according to the wall thickness required. The inner and outer surfaces of these specimens were covered with self-adhesive vinyl acetate strips. The model specimens were then compressed by 10 % in the same testing apparatus at a speed appropriate to their dimensions. During the compression both the manner and the temporal succession of the failure forms, particularly folding, were observed. On the outer surface of the tested specimens the shape, dimension and number of folds were then measured, analysed statistically and compared with the fold formations in the wood cells.

Terminology

General Description

The wood samples tested in axial compression show two groups of destruction, i.e., failure regions and cracks, both of varying sizes. The failure regions extend layer-like throughout the tissue and are composed of structural deformations. The edge of the failure regions appears on the longitudinal surface of the specimen as failure lines of varying, well measurable widths and of different inclination to the longitudinal axis of the sample (Figs. 5, 6, 25, 30). On the transverse surface they appear as failure areas of varying dimensions extending beyond the specimen limits and of diverse forms (Figs. 7, 8, 27, 32). The failure regions may be roughly divided into the macroscopic (visible to the naked eye) and the microscopic; accordingly on the longitudinal surfaces macroscopic and microscopic compression lines can be observed. The deformations found in the cells and tissues are telescopic shortening and buckling. The telescoping occurs mainly in thin-walled elements and is characterized by the formation of coarse transverse folds and longitudinal cracks in the inner cell-wall layers (Figs. 17, 19). Buckling chiefly affects the thick-walled wood cells, which are thereby diverted from their natural axial orientation. The buckling is accompanied by fine wrinkling, which may be transversal or longitudinal, or both, and by cracks in the middle lamella and/or adjacent cell-wall layers and sometimes by defibrillation of the secondary wall (Figs. 18, 20). The cracks usually run in the axial direction; transverse cracks are infrequent. The macroscopic cracks (those visible to the naked eye) usually separate tissues with different deformation behaviour. The microscopic cracks penetrate individual tension or shear stressed cell-wall layers or – less frequently – whole cell-walls. The orientation of the cracks always conforms to rule, the size is more a matter of chance.

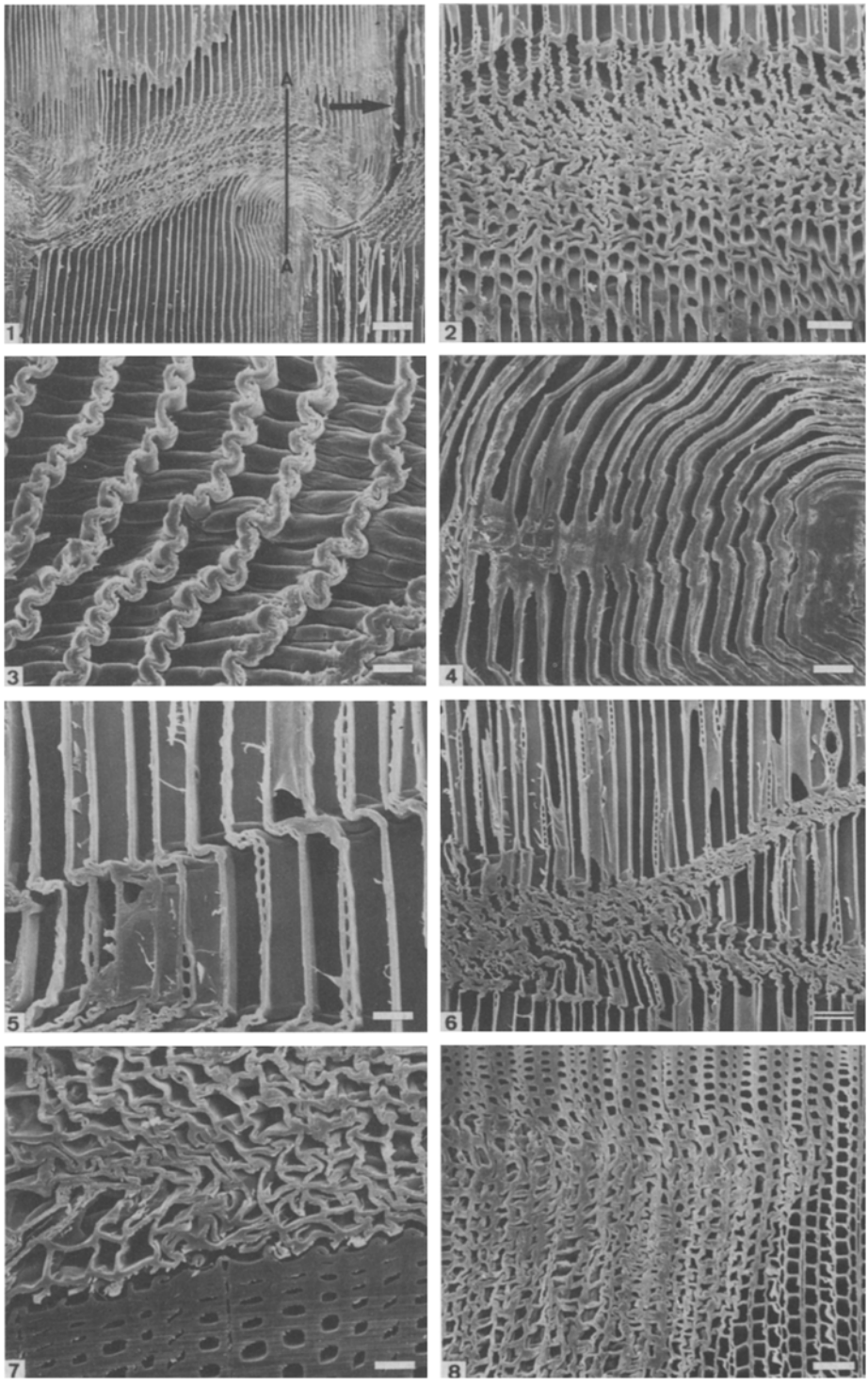
A
A
1
2
3
4
5
6
7
8

Categories

Most of the previous investigations were concerned with the wood of spruce (*Picea* spp.) which is quite justified when its importance in building is taken into consideration. The structural changes examined under the microscope were chiefly the slip planes. The reason for this is that most of the investigations were carried out under a light microscope in polarized light, a method eminently suitable for such observations. SEM investigations are described in papers by Keith (1971, 1974) with *Picea glauca* (Moench) Voss, by Scurfield et al. (1972) on 17 Australian species, by Delorme and Verhoff (1975) with *Picea abies* Karst and by Kitahara et al. (1981) with *Cryptomeria japonica* D. Don. A definite identification of the well-known slip planes is rather difficult in the SEM (Scurfield et al. 1972; Delorme, Verhoff 1975). The nomenclature based on investigations under the light microscope was revised several times (Kisser, Steininger 1952; Dinwoodie 1968; Keith, Côté 1968) and supplemented by suggestions from Scurfield et al. (1972) to include SEM observations, but the existing differences have not yet been resolved. The reason probably lies in the difficulty of defining exact categories referring to a continuous process of changes. Our account is based on the following progressive classification of the structural deformations:

1. Stress lines or thrust lines (Spannungslinien).

Horizontal or slightly inclined wrinkling in the cell-wall towards the cell-lumen, affecting the innermost layers of the secondary cell-wall or the so-called "cell-wall lining" according to Scurfield et al. (1972) only (Fig. 11).

2. Slip planes, slip lines (Gleit-, Scher-, Stauch- or Verschiebungslinien).

Locally restricted dislocation or cringkkling of the cellulose fibrils in the whole of the cell-wall of one or two neighbouring cells, without any prominent change in the shape of the cell (Fig. 12).

Fig. 1. Spruce. Wavy course of a macroscopic compression failure line. Arrow points to crack in the growth ring boundary. RLS, SEM, x 30, scale mark = 200 μm

Fig. 2. Spruce. Surface corresponding to the section A-A in Fig. 1. From top to bottom transition from the early- to the latewood zone. TLS, SEM, x 60, scale mark = 100 μm

Fig. 3. Spruce. Telescopic shortening and lateral displacement of compressed earlywood tracheids through fold formation in the radial and tangential cell walls. RLS, SEM, x 280, scale mark = 20 μm

Fig. 4. Spruce. Buckled latewood tracheids bent in radial direction. RLS, SEM, x 110, scale mark = 50 μm

Fig. 5. Spruce. Inclined microscopic compression failure line. Note the course of the failure line as related to the ray arrangement. TLS, SEM, x 115, scale mark = 50 μm

Fig. 6. Spruce. Macroscopic failure line with branching. TLS, SEM, x 55, scale mark = 100 μm

Fig. 7. Spruce. Compression failure area in earlywood with strongly deformed tracheids and tangential crack formation at the growth ring boundary. TS, SEM, x 115, scale mark = 50 μm

Fig. 8. Spruce. Failure area in the middle part of a growth ring. TS, SEM, x 60, scale mark = 100 μm

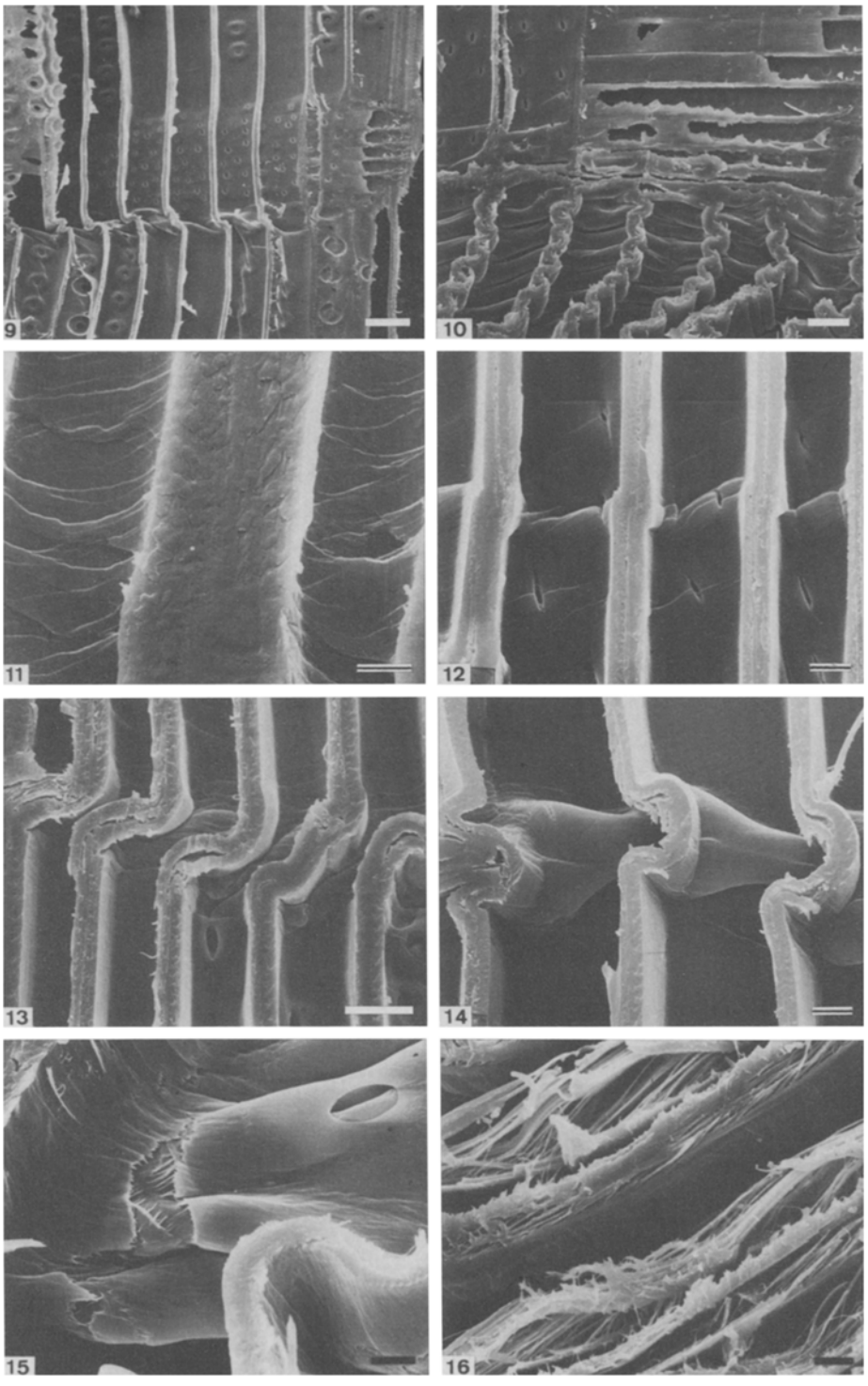
9
10
11
12
13
14
15
16

3. Microscopic compression failure lines or creases (Mikroskopische Bruchlinien). Microscopically visible changes in the cell shape through lateral buckling and/or telescopic shortening (Figs. 5, 29). A double bending of the cell-wall leads to the formation of type S (Fig. 13) and a triple one to type U (Fig. 14). The microscopic compression failure lines are usually connected with the occurrence of stress lines and slip planes.

4. Macroscopic compression failure lines or creases (Makroskopische Bruchlinien). Deformation region visible to the naked eye; a multi-layered qualitative and quantitative accumulation of the structural deformation patterns. In contrast to the short microscopic compression failure lines with random orientation, the longer macroscopic ones show regular inclinations (horizontal or slightly inclined in the radial plane and at 50–65 ° to the grain in the tangential plane and frequent branching (Figs. 1, 6, 25, 30).

Results

Spruce

The macroscopic failure regions are regular; in the radial plane of the specimen the failure lines form characteristic horizontal waves with a fairly straight part in the earlywood and a curved part in the latewood (Fig. 1); in the tangential plane they are often straight lines with varying angles of inclination and frequent branching (Fig. 6). The width of the failure lines remains constant in the radial plane (Fig. 1), while in the tangential one it is variable, particularly where there is branching (Fig. 6). Its values vary between 200 and 900 μm. On the transverse specimen surface the failure areas are

---

Fig. 9. Spruce. Microscopic failure line at the edge of an unmodified ray in earlywood. RLS, SEM, x 120, scale mark = 50 μm

Fig. 10. Spruce. Macroscopic compression failure line at the edge of a slightly compressed ray in earlywood. RLS, SEM, x 300, scale mark = 20 μm

Fig. 11. Spruce. Horizontal to slightly inclined wrinkles on the inner surface of the cell wall in latewood tracheids, regarded as stress lines. RLS, SEM, x 1520, scale mark = 5 μm

Fig. 12. Spruce. Fine failure line in the cell wall of neighbouring latewood tracheids, regarded as an accumulation of slip planes. RLS, SEM, x 580, scale mark = 10 μm

Fig. 13. Spruce. S-shaped buckling in the cell walls of neighbouring latewood tracheids form a microscopic failure line. Note the separations in the middle lamella and/or adjacent cell wall layers in the bent area. RLS, SEM, x 480, scale mark = 20 μm

Fig. 14. Spruce. U-shaped cell wall buckling in neighbouring tracheids forming a microscopic failure line. TLS, SEM, x 560, scale mark = 10 μm

Fig. 15. Spruce. Longitudinally orientated crack in the cell wall of an earlywood tracheid. Note the undamaged bordered pit. RLS, SEM, x 1210, scale mark = 5 μm

Fig. 16. Spruce. Defibrillation of the cell wall of a sharply bent late wood tracheid. RLS, SEM, x 1100, scale mark = 5 μm

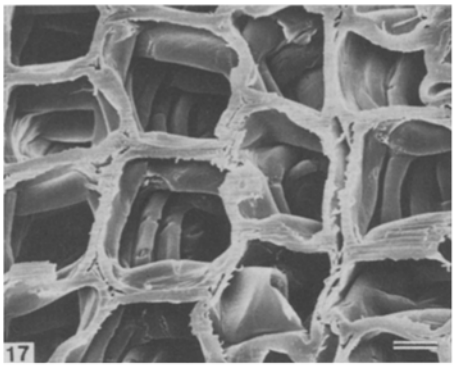
17

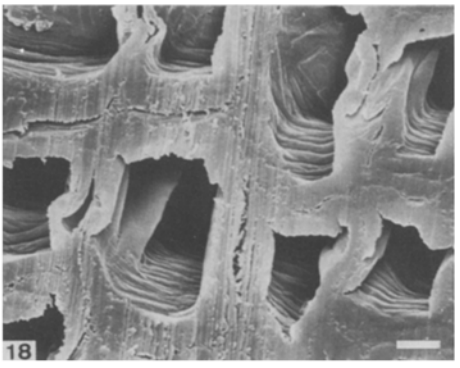
18

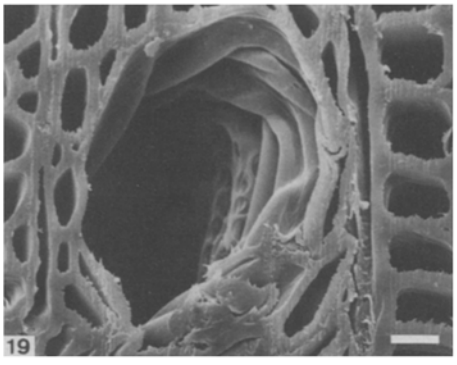
19

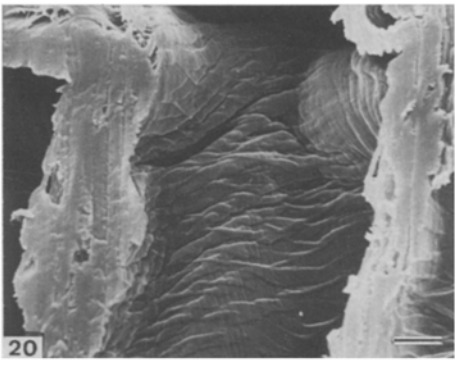
20

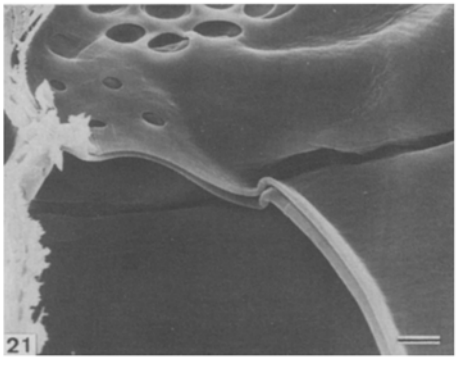
21

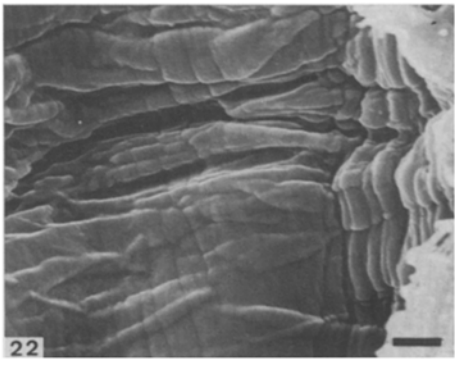
22

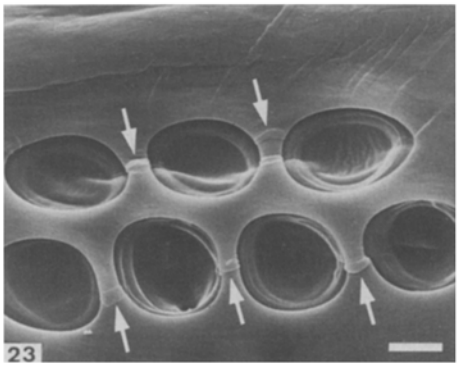
23

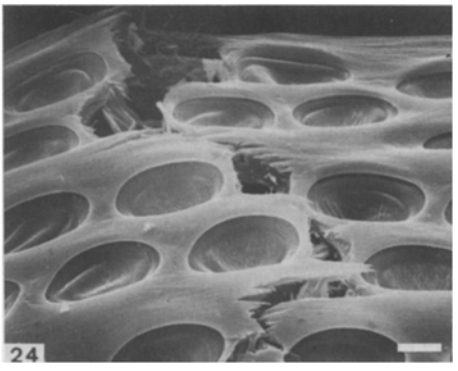
24

irregularly distributed, and in form largely oval in the earlywood and tangentially elongated in the latewood; their size is variable (Fig. 8). The microscopic failure regions are often found at the ray margins (Fig. 9). The failure lines are between 10 and 40 μm wide (Fig. 5) and belong either to type S (Fig. 13) or type U (Fig. 14). The slightest deformation that can be found microscopically represents the wrinkling on the inner surface of the cell-wall (Fig. 11), a phenomenon also found occasionally in the control samples. This wrinkling may be related to the stress lines as described by Kisser and Steininger (1952). We assume the fine failure lines in Fig. 12 to be a series of slip planes.

The growth rings show a differentiated pattern of deformation and fracture: earlywood is compressed (Fig. 3), while latewood is buckled (Fig. 4), the transition from one kind of deformation to the other running continuously in the growth ring. Latewood represents the load bearing zone under axial compression while earlywood takes over the role of stress distribution and cushioning. This differentiation is apparent particularly on the radial longitudinal surface (Fig. 1). On the tangential longitudinal surface cushioning and buckling often merge as a result of the wavy nature of the failure regions (Fig. 2). The growth ring boundary apparently produces a discontinuity, for here the dense latewood with its tendency to buckle borders directly on the light earlywood zone with different failure characteristics. This gives rise to shear forces, resulting in macroscopic cracks at the growth ring boundaries (Figs. 1, 7).

The earlywood tracheids are heavily distorted by the compression forces, whereby the cell-walls fold, protruding into the cell lumen (Figs. 3, 17). The thickness of these folds varies from 10–30 μm (Fig. 3). In connection with the buckling of the latewood, the earlywood tracheids collapse particularly in the radial direction. The most stable regions of a cell seem to be located at the corners (Fig. 7). In addition a slight deflexion and/or displacement of the tracheids occurs in the tangential direction (Fig. 6). On the convex surface of the folds, caused by telescoping, microscopic cracks occur, most of

---

Fig. 17. Spruce. Telescoping and fold formation in the radial and tangential cell walls of earlywood tracheids. TS, SEM, x 300, scale mark = 20 μm

Fig. 18. Spruce. Wrinkling in the cell wall of latewood tracheids. TS, SEM, x 580, scale mark = 10 μm

Fig. 19. Aspen. Telescoping and fold formation in a vessel wall. TS, SEM, x 310, scale mark = 20 μm

Fig. 20. Aspen. Wrinkling across the cell axis in the cell wall of a libriform fibre. RLS, SEM, x 1210, scale mark = 5 μm

Fig. 21. Aspen. Course of a microscopic failure line across a vessel perforation plate. RLS, SEM, x 560, scale mark = 10 μm

Fig. 22. Aspen. Wrinkle fields orientated transversely and longitudinally to the cell axis in the cell wall of a libriform fibre. RLS, SEM, x 3120, scale mark = 2 μm

Fig. 23. Aspen. Vessel – to – ray pitting. Note the compression lines on the axially orientated pit margins (arrows). RLS, SEM, x 1400, scale mark = 5 μm

Fig. 24. Aspen. Vessel – to – ray pitting. The crack formation runs consistently between the pits. RLS, SEM, x 1150, scale mark = 5 μm

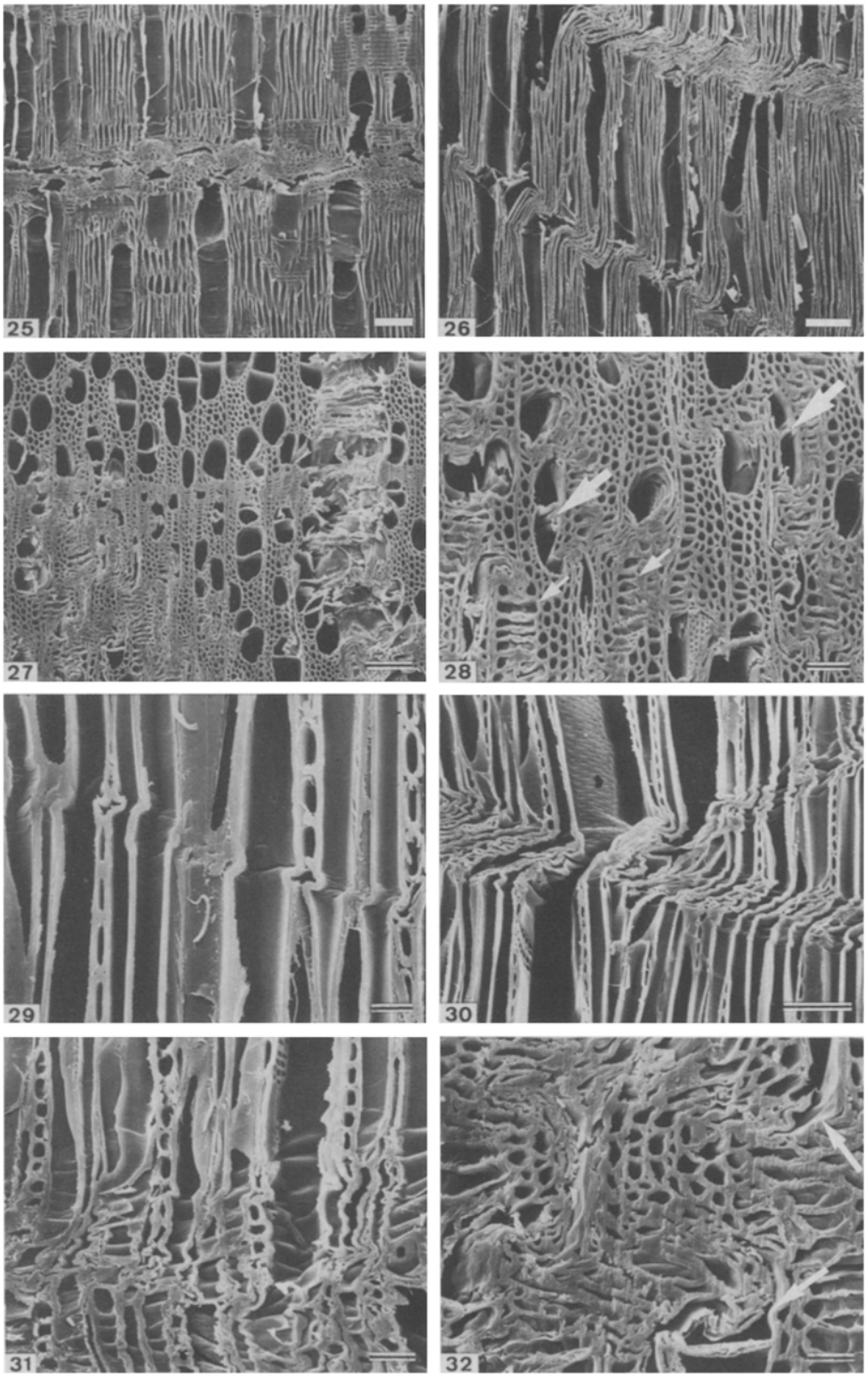
25
26
27
28
29
30
31
32

them axially orientated (Fig. 15), indicating where transverse tensile stress arises in the tissue under compression loading. The cracks usually affect only the innermost layer of the secondary wall (S_3). The destructions are greatest in the centre of the deformation regions and their extent diminishes continuously towards the periphery. The bordered pits remain undamaged even in the most deformed tracheids (Fig. 15). The tracheids of the latewood buckle chiefly in the radial direction (Fig. 1) and to a lesser extent in the tangential. The diameters of the bend are 400–500 μm in the radial direction (Fig. 4) and in the tangential it is variable. On the inner surface of the cell wall fine transversely orientated wrinkling may be observed with a thickness of 1–4 μm in the longitudinal direction (Fig. 18). When the latewood tracheids are sharply bent, separations can occur in the middle lamella and/or adjacent cell-wall layers induced by shear stresses (Fig. 13) and at times defibrillation can be seen in badly damaged tracheid walls (Fig. 16). The rays appear to strongly resist the deforming force: the microscopic failure lines are often (Fig. 9) and the macroscopic ones sometimes at the ray margins (Fig. 10), without the actual rays being affected. It seems as if the ray constitutes a wedge, across the edge of which the tracheid wall slides by. Several axial and radial resin canals are found in the deformation regions without any notable changes, an indication of the great stiffness of this element.

Aspen

In this species the macroscopic deformation regions are less regular than in the spruce. The failure lines run horizontally or slightly inclined on the radial longitudinal surface (Fig. 25) and are more steeply inclined in the tangential one (Figs. 26, 30). The widths of the failure lines vary along their course in both the radial and the tangential longitudinal surfaces between 100 and 600 μm. Branchings are frequent on both surfaces

---

Fig. 25. Aspen. Transversely orientated macroscopic failure line. RLS, SEM, x 25, scale mark = 200 μm

Fig. 26. Aspen. Macroscopic failure lines running parallel to each other and oblique to the grain. TLS, SEM, x 30, scale mark = 200 μm

Fig. 27. Aspen. One radially extended and one concentric failure area. TS, SEM, x 30, scale mark = 200 μm

Fig. 28. Aspen. Section from the periphery of a failure area. Note the tangentially orientated buckling of the fibres (slender arrows) and the consequent deformation of the vessels in the same direction (broad arrows). TS, SEM, x 60, scale mark = 100 μm

Fig. 29. Aspen. Inclined microscopic failure line. TLS, SEM, x 300, scale mark = 20 μm

Fig. 30. Aspen. Branching macroscopic failure line. TLS, SEM, x 95, scale mark = 100 μm

Fig. 31. Aspen. Fold formation in the vessel and fibre walls at the periphery of a macroscopic failure line. TLS, SEM, x 130, scale mark = 50 μm

Fig. 32. Aspen. Section from the centre of a failure area. Note the tangentially buckled fibres and the entirely compressed vessels (arrows). TS, SEM, x 130, scale mark = 50 μm

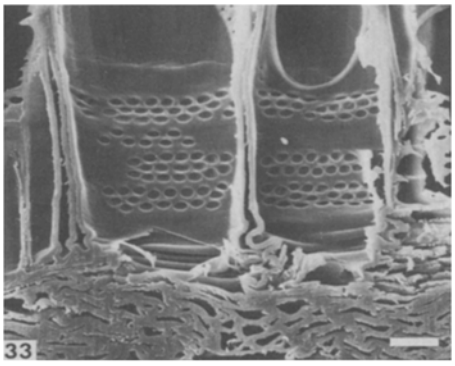
33

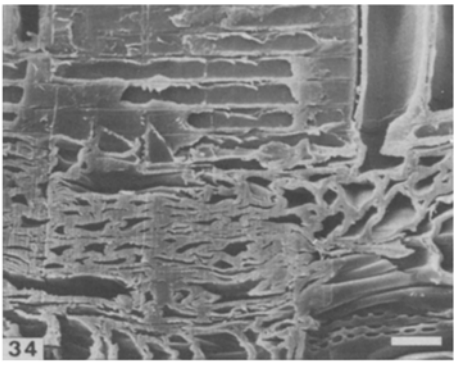
34

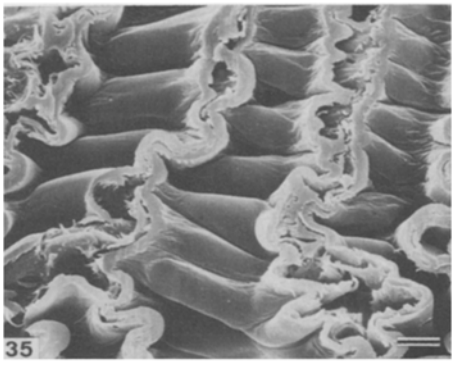
35

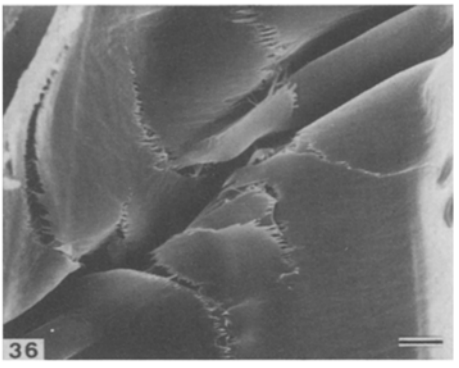
36


37

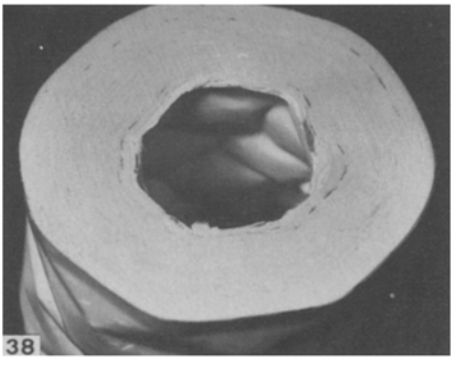
38

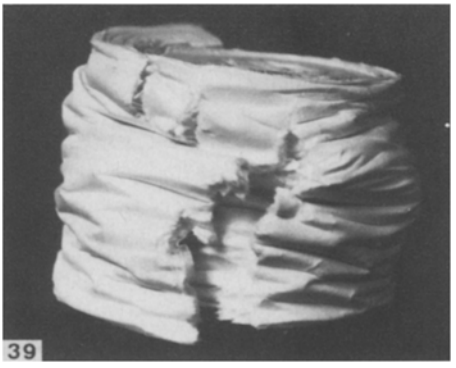
39

(Fig. 30). The greatest destruction again occurs in the centre of the failure regions, decreasing in severity towards the periphery. On the transverse surface the failure areas are irregularly distributed. The forms may be round to oval and radially elongated (Figs. 27, 28). The microscopic failure regions are more frequent than in spruce. On the longitudinal surfaces the microscopic failure lines are often found as outrunners from the macroscopic ones and on the radial surfaces they are often at the ray margins (Fig. 34). Their width is 15–30 μm (Fig. 29).

There is a homogeneous pattern of deformation and crack occurrence throughout the growth rings (Fig. 27). The tissue buckles in the tangential direction (Figs. 26, 30) concurrently with the formation of macroscopic cracks in the radial direction. The radius of curvature in the tangential buckling is decidedly variable and clearly influenced by the distance between the vessels (Figs. 26, 30).

The vessels show characteristic telescoping with fold formation. The folds are 10 to 45 μm thick and run circumferentially (Fig. 19). The vessels are bent, together with portions of fibre tissue, in the tangential direction and become compressed in the same direction (Figs. 28, 32). On the convex surface of the folds, cracks occur, but they usually affect only the S_3 layer, seldom the whole cell wall (Fig. 36). The cracks are mainly axially orientated and have typically "frayed" edges. The vessels – to – ray pitting does not seem to induce any weakening of the vessel wall (Fig. 33); nor are there any torn pit apertures. On the contrary, the cracks run between the pits (Fig. 24). The pit margins with their vertical orientation often show fine compression lines (Fig. 23). The few vessel perforation plates that were examined indicate a high elasticity (Fig. 21). The fibres buckle mostly in the tangential direction and become compressed and sometimes bent radially (Fig. 30). Compression folds are more often found on the periphery of the failure region than in the centre (Fig. 31); the width of the folds ranges between 5 and 20 μm (Fig. 35). On the inner surface of the cell wall fine wrinkles can be seen, with a width of 1 to 6 μm (Fig. 20). They are arranged in a parallel manner in wrinkle fields, usually running across the cell axis, but there are also some longitudinal wrinkle fields, as well as combinations of both, indicating a change

---

Fig. 33. Aspen. Macroscopic failure line in direct proximity to undamaged pit fields. RLS, SEM x 130, scale mark = 50 μm

Fig. 34. Aspen. Macroscopic failure line at a ray margin. RLS, SEM, x 135, scale mark = 50 μm

Fig. 35. Aspen. Fold formation in compressed libriform fibres and separations in the middle lamella and/or adjacent cell wall layers. TLS, SEM, x 560, scale mark = 10 μm

Fig. 36. Aspen. Crack formation in the cell wall of a vessel. TLS, SEM, x 590, scale mark = 10 μm

Fig. 37. Axially compressed tube-like model specimen of paper. The folds arise perpendicular to the direction of the compression force and are arranged in a helical pattern. Macro-photograph

Fig. 38. View into the lumen of the specimen in Fig. 37. The folds arch towards the lumen. Macro-photograph

Fig. 39. Axially compressed paper model specimen. Cracks arise as a result of transverse tensile stresses and affect groups of lamellae or penetrate the whole wall. Macro-photograph

of stress direction during the course of deformation (Fig. 22). In the fibres that are sharply folded or bent, shear separations occur in the middle lamella and/or adjacent cell wall layers (Fig. 35). The simple slit-shaped pits usually remain undamaged. The compression failure lines are often found at the ray margins (Fig. 34).

Comparison Between Spruce and Aspen

Similarities in the deformation pattern are found at macroscopic, cellular and submicroscopic levels. In both species there are macroscopic and microscopic failure regions with telescoping and buckling at all levels. The failure lines and areas are similar in frequency, course and extent. Microscopic and macroscopic cracks can be observed in both species, but there are differences in the orientation of the latter. Cells with a wide lumen – such as earlywood tracheids and vessels – show telescopic shortening and folds, and the dimension of the folds is similar. Cells with a narrow lumen – latewood tracheids and fibres – tend rather to buckle. The fibres additionally show a tendency to telescoping and fold development. The perforations have not proved to be a weak point of the cell wall. On the inner surface of heavily buckled cells there are transverse fold systems, and the middle lamella and/or adjacent cell wall layers show separations when the radius of the curvature is small. The trans-wall failures are mainly axially orientated and do not usually extend beyond the S_3 layer. In both species the ray margins are the place where the failure lines most often occur, but the rays themselves are seldom deformed. The formation of the macroscopic and microscopic failure regions in the tissue and also the failure behaviour of the cell wall appear to follow the same mechanism in both species, whereas the deformation pattern of the individual cells is dependent on the cell type.

An essential difference between the two species arises from the specific growth ring structures. The failure forms of the earlywood and the latewood zones of spruce are clearly distinguishable, while those of aspen remain quite homogeneous throughout the growth ring. The macroscopically visible buckling of the tissue takes place in the tangential direction in both species, except in the latewood of the spruce where the buckling mainly occurs in the radial direction. In spruce macroscopic cracks arise in the tangential plane but, in aspen in the radial plane. The reason for this difference may be found in the different growth ring structure of the two species. The increment of spruce may be regarded as lamellated in two ways: tangentially as a result of the alternation of light earlywood and dense latewood zones, and radially as a result of the ray system. The deformations follow both lamellae systems. In the highly homogeneous aspen growth rings, there is only a radial structuring formed by the rays. Thus, the weak points are the growth ring boundaries in the spruce and the boundary surface between the rays and the ground tissue in both species. Other differences observed may perhaps be accidental; they concern the occurrence of defibrillation in the latewood tracheids of the spruce and the combination of transverse and vertical folds in the aspen fibres.

Model Specimens

The model experiments provide a direct observation of the formation of failure and its development in samples which in their tube-like shape, their wall portions and their layered wall construction have a certain similarity with axial cell segments. On the other hand, these model specimens lack the wall perforations, the matrix substance binding the lamellae together and the internal anisotropy of the individual lamellae, all of which are decisive for the stability of the wood cells. During and after the longitudinal compression of the model specimens the following observations were made. As one of the typical destruction forms of the tube wall, rhomboid folds are seen running across the longitudinal axis (Fig. 37) projecting into the tube lumen (Fig. 38). Thus the reduction in the length of the specimen under the load does not alter the external diameter. Cracks do not occur until the reduction in specimen length reaches a stage where the wall folds fill the whole lumen of the tube. They always arise parallel to the axis across one or more folds in the longitudinal direction, and starting on the outside they traverse groups of lamellae or the entire wall (Fig. 39). The folds form in rows, starting from the side where the flexible yoke of the testing machine is located. In the smallest, thin-walled test specimens, the whole destruction consists of folds on the side of the load application. The size of the folds increase with the increasing dimensions of the specimens, but it remains constant over the entire length of the same specimen. The density of the folds on the surfaces is closely correlated with the dimensions of the specimens (Fig. 40): in thin-walled specimens the folds are less numerous than in

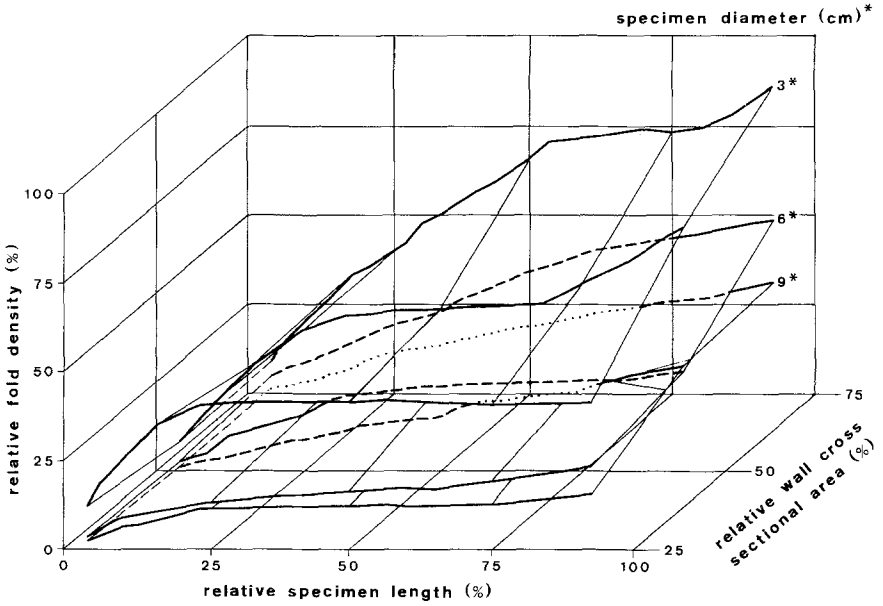

Fig. 40. Frequency distribution of the cumulative relative fold density (%) on the surface of the model specimens, depending on the specimen dimensions (cm) and the proportions of wall (%)

the thick-walled ones, but this is counterbalanced by more frequent buckling inwards and tipping outwards. As the specimen dimensions decrease, there is a non-linear increase in the density of the folds, so that a high incidence of folds must be expected in the smallest specimens as in the wood cells.

Comparison Between Wood and Model Specimens

The deformation in the xylem cells correspond to many of those in the model specimens. Typical of the destruction phenomena are the transverse or slightly inclined folds forming depressions towards the lumen of the specimens. Cracks are axially orientated; they do not occur until an advanced stage of destruction is reached and they are often confined to single wall layers. In any one specimen the dimensions of the folds remain constant over its whole length. The size of the folds correlates positively with the overall diameter of the specimen. The frequency of the folds is most strongly influenced by the thickness of the walls, being greater in the thick-walled specimens than in the thin-walled ones. These correlations indicate that the deformation behaviour of the xylem cells – but not that of tissues – may be partly explained by their geometry.

Discussion

The axial strength of wood is of great importance both biologically and technically. It is one of the mechanical properties most subject to stress both in the living tree and in wood constructions. The axial compression strength is only about half as great as the tensile strength, so the failure of wood under compression is more frequent. The special feature of the failure process under axial compression load is that structural changes are continuously arising and developing. Simultaneous elastic and plastic form changes characterise the statically unstable system of the wood structure even when the axial compression load is relatively low. The first slight permanent structural changes – slip planes – in spruce occur according to Kisser and Steininger (1952) at about 50 % of the failure load. In later investigations Dinwoodie (1968) set this limit as low as 25 % and Keith (1971) as high as 60–70 % of the ultimate strength. The failure process can only be correctly interpreted when the structural changes are understood. When the changes are described there is always the danger of artefacts, as was recognised at an early date by Robinson (1920). These deformations may be divided into three groups, according to the time period when they occur: a) on the living tree, caused by gales, storms or the weight of snow (cf. Kisser, Steininger 1952; Delorme, Verhoff 1975) or during the transport and treatment of the raw wood, b) during experimental preparation (Kisser, Steininger 1952; Keith, Côté 1968) and c) during the actual experiment. In order to avoid artefacts and false interpretations it is necessary to adopt certain measures: a) to carry out combined macroscopic and microscopic investigations, b) to make control tests on unaltered material, using the same prepara-

tive methods as in the experiment and c) to use preparation in air dry or dry condition, to avoid swelling of the samples.

The differences in failure pattern between the earlywood and the latewood in spruce, which we have described here, conform to the findings of Stupnicki (1970) and Delorme and Verhoff (1975). However, the theory postulated by Frey-Wyssling (1953) that the tissue buckling is predominantly in the tangential direction must – at least as far as the spruce is concerned – be refuted. The role of the rays in the deformation process has often been discussed. Grossmann and Wold (1971), Grossmann (1974) and Delorme and Verhoff (1975) point out that the rays have a stabilising effect on the axial tissues in the radial direction which therefore favour tangential buckling. The boundary areas between the rays and the axially orientated ground tissue are seen as weak points at which the first structural changes occur (Keith, Côté 1968; Dinwoodie 1968; Scurfield et al. 1972; Delorme, Verhoff 1975). Keith (1971, 1974) defined the weak point more precisely as the ray margins. Our observations confirm this statement. At the same time the rays appear to be more resistant to the axial load itself than the ground tissue. However, an influence of the ray arrangement on the course of the macroscopic compression failure lines has been denied (Wardrop, Addo-Ashong 1965). In our opinion, rays do have a locally limited influence at least upon the course of the microscopic failure lines. The influence of the different kinds of pits and of the vessel perforations cannot always be definitely settled. The bordered pits in particular seem to have a very stable structure, which may be explained by the circular arrangement of the fibrils in the pits. Whether the ray traces really are a weak point, as Scurfield et al. (1972) assume, is not clear from our investigations. The same authors describe the spread of transwall failure from the slit-like simple pit apertures in fibres, which we have observed in a few cases in our material, without being able to establish any rule about it.

In the process of failure upon axial compression, deformations are clearly the most frequent change and cell wall cracks are relatively less so. Of the two types of cracks the inter-wall failure is more frequent than the trans-wall failure, the latter often being confined to one or a few layers of the secondary wall. On the question as to which cell wall layer plays the most important part under load there are differences of opinion. Stupnicki (1970) calculates that the middle lamella contributes to 95 % to the strength of the wood parallel to the grain. But Jeronimidis (1976) emphasises the essential part played by the S_2-layer of the secondary wall in the fracture process upon longitudinal tension. Several authors (Wardrop, Addo-Ashong 1965; Keith, Côté 1968; Delorme, Verhoff 1975) describe the layer boundary S_1-S_2 of the secondary wall as the place where intra-wall failure arises as a result of shear strains. Scurfield et al. (1972) express doubts about this. On the other hand Debaise et al. (1966) and Borgin et al. (1975) see the region of the middle lamella and the primary wall as predisposed for failure, while Ohsawa and Yoneda (1978) find crack formation in all the layer boundaries of the cell wall under shear load. It seems to us that these divergent opinions must be traced back to differences in both materials and methods, so that a uniform pattern of failure cannot be expected.

Looking to the future, we should very much like to see some efforts made towards a definite clarification of the nomenclature in the field of stress lines and slip planes through combined light microscope and SEM investigations. These investigations should also be extended to other species of wood, with particular attention paid to species with ring porous vessel arrangement, multiseriate rays, with bound parenchyma tissue.

References

Borgin, K.; Parameswaran, N.; Liese, W. 1975: The effect of aging on the ultrastructure of wood. Wood Sci. Technol. 9: 87–98

Debaise, G. R.; Porter, A. W.; Pentoney, R. E. 1966: Morphology and mechanics of wood fracture Mater. Res. Stand. 6: 493–499

Delorme, A.; Verhoff, S. 1975: Zellwanddeformationen in sturmgeschädigtem Fichtenholz unter dem Rasterelektronenmikroskop. Holz Roh- Werkst. 33: 456–460

Dinwoodie, J. M. 1968: Failure in timber. Part 1: Microscopic changes in cell wall structure associated with compression failure. J. Inst. Wood Sci. 4: 37–53

Dinwoodie, J. M. 1975: Timber – a review of the structure – mechanical property relationship. J. Microsc. 104: 3–32

Ellenberg, H.; Klötzli, F. 1972: Waldgesellschaften und Waldstandorte der Schweiz. Mitteilung. Eidg. Anstalt f. d. forstl. Versuchswesen. 48: 591–868

Exley, R. R.; Butterfield, B. G.; Meylan, B. A. 1974: Preparation of wood specimens for the scanning electron microscope. J. Microsc. 101: 21–30

Frey-Wyssling, A. 1953: Über den Feinbau der Stauchlinien in überbeanspruchtem Holz. Holz Roh-Werkstoff 11: 283–288

Grossmann, P. U. A. 1974: The role of the botanical structure of wood in the fracture process. In: Proceedings of the Australian Fracture Group Conference, Melbourne: 51–57

Grossmann, P. U. A.; Wold, M. B. 1971: Compression fracture of wood parallel to the grain. Wood Sci. Technol. 5: 147–156

Jeronimidis, G. 1976: The fracture of wood in relation to its structure. Leiden Bot. Ser. 3: 253–265

Keith, C. T. 1971: The anatomy of compression failure in relation to creep-inducing stresses. Wood Sci. 4: 71–82

Keith, C. T. 1974: Longitudinal compressive creep and failure development in white spruce compression wood. Wood Sci. 7: 1–12

Keith, C. T.; Côté, W. A. Jr. 1968: Microscopic characterization of slip lines and compression failures in wood cell walls. For. Prod. J. 18: 67–74

Kisser, J.; Steininger, A. 1952: Makroskopische und mikroskopische Strukturänderungen bei der Biegebeanspruchung von Holz. Holz Roh-Werkstoff 10: 415–421

Kitahara, R.; Tsutsumi, J.; Matsumoto, T. 1981: Observations on cell wall response and mechanical behaviour in wood subjected to repeated static bending load. Mokuzai Gakkaishi 27: 1–7

Kučera, L. J. 1981: Cutting wood specimens for observations in the scanning electron microscope. J. Microsc. 124: 319–325

Ohsawa, J.; Yoneda, Y. 1978: Shearing test of woods as a model of defibration. Part 2: Exposed surface by shearing fracture. Mokuzai Gakkaishi 24: 790–796

Robinson, W. 1920: The microscopical features of mechanical strains in timber and the bearing of these on the structure of the cell wall in plants. Philos. Trans. Soc. London. Ser. B. 210: 49–82

Scurfield, G.; Silva, S. R.; Wold, M. B. 1972: Failure of wood under load applied parallel to grain: A study using scanning electron microscopy. Micron 3: 160–184

Stupnicki, J. 1970: Strukturmodell der Holzzelle zur Untersuchung von Bruchvorgängen. Holztechnologie 11: 168–176

Wardrop, A. B.; Addo-Ashong, F. W. 1963: The anatomy and fine structure of wood in relation to its mechanical failure. In: C. J. Osborn (ed.) Fracture. Proceedings of the First Tewksbury Symposium. Melbourne: 169–200

(Received December 14, 1981)

Dr. L. J. Kučera
P. D. Dr. M. Bariska
Institut für Wald- und Holzforschung der ETH
ETH-Zentrum
CH-8092 Zürich
Schweiz

Book Review

Kirk, T. K.; Higuchi, T.; Hou-Min Chang (ed.): Lignin Biodegradation: Microbiology, Chemistry, and Potential Applications. Vol. I, 241 pp., Vol. II, 255 pp. Boca Raton, Florida: CRC Press 1980. Vol. I: US $ 66.95. Outside US $ 76.95. Vol. II: US $ 69.95. Outside US $ 79.95

The biodegradation of lignin is a very complex process because of the irregular structure of the substrate and the complicated interaction between the various microorganisms and enzyme systems involved. It is therefore not surprising that, in spite of many years' work, the understanding of the process is still incomplete. During the past two decades, results from studies of the biosynthesis of lignin and its analytical composition have led to a fairly good insight into the structural features characteristic of this natural polymer. This has made possible increased research efforts in the field of lignin biodegradation with the aim of elucidating the role of lignin in the earth's carbon cycle and, hopefully, also finding industrial applications for ligninolytic systems. Considerable progress has been made in the past 7–8 years and valuable results continue to be reported at a steadily increasing rate. As is true of all rapidly developing areas, there is a great need for collecting and summarizing the results obtained at certain intervals.

The international seminar on lignin biodegradation, held in May 9–11, 1978 at the US Forest Products Laboratory in Madison, Wisc., filled this need very well. A group of 43 researchers met to present their results, including their unpublished work, and to define the state-of-the-art in this field. The proceedings of this seminar have been collected in the present two volumes containing 11 and 16 chapters, most of them written by widely recognized experts. The three subject areas indicated in the book's title are well covered by the contributions.

After a short review of the biosynthesis and morphological distribution of lignin (Chapter 1), the microbial catabolism of lignin-related aromatic compounds is summarized (Chapter 2). Following these two introductory chapters, modern methodology in the study of lignin biodegradation using ^{14}C-labelled synthetic and natural lignins is described in Chapter 3. This method of isotope labelling of the substrate is employed in some of the following papers dealing with the chemistry of soil humus formation (Chapter 4) and the degradation of lignin by micro- and macrofungi and by bacteria (Chapter 6). Remarkable progress in the elucidation of the chemistry of the lignin biodegradation is reported in the last four chapters of Vol. I. These are concerned with the microbial degradation of dehydrogenation polymerizates (DHPs) (Chapter 8) and of dilignols (Chapter 9) from coniferyl alcohol, with stereobiochemical aspects of the degradation process (Chapter 10), and with the characterization of lignin isolated from wood decayed by white-rot fungi (Chapter 11).

The importance of phenol oxidases and the possible role of cellobiose: quinone oxidoreductase in the microbial degradation of lignin is the subject of the first three chapters of Vol. II. Various culture parameters important for the development of ligninolytic activity are discussed in Chapter 4, and a genetic method for selecting mutants with high lignin degradation capacity is